Charge Order in the Blume-Capel Model on a Triangular Lattice

Matthew Nelson,[1] Bianca Pol,[2] Eduardo Ibarra-García-Padilla,[3,4] Richard Scalettar,[4] and Matthew Enjalran[5]

[1]*Kalamazoo College*
[2]*University of Chicago*
[3]*San José State University*
[4]*University of California, Davis*
[5]*Connecticut State Colleges and Universities Center for Nanotechnology, Southern Connecticut State University*

We use classical Monte Carlo methods to investigate antiferromagnetic order in the Blume Capel model on a triangular lattice. We demonstrate that a finite temperature transition to an AFM ordered phase occurs at a T_c dependent on chemical potential D. This ordered phase is an occupied bipartite honeycomb sublattice of the full triangular lattice. This is a classical analog of several real-world materials.

INTRODUCTION

Strongly correlated materials exhibit charge and magnetic ordering, where a relevant question is how geometric frustration affects them. These systems are described by fermionic Hamiltonians, which are very difficult to study numerically and thus it is difficult to determine a mechanism responsible for the observed charge and spin orders. For those reasons, in this work we numerically study the classical Blume Capel (BC) model in a triangular lattice in order to capture the essential features of a charge and spin ordered system in a geometrically frustrated lattice. We use classical Monte Carlo methods to investigate both antiferromagnetic and charge order in the BC model and compare against a previously reported renormalization group (RG) calculation. To determine the presence or absence of each type of order, we construct and utilize novel non-local order parameters that couple to the charge and spin degrees of freedom. We demonstrate the existence of an antiferromagnetically ordered and charge ordered phase in which spins occupy only a honeycomb sublattice of the full triangular lattice, whose bipartite structure avoids magnetic frustration. Although our results are consistent with RG regarding the location of the finite temperature second- and first- order phase boundaries from the paramagnetic to magnetic phase in the temperature vs chemical potential plane, we detect a richer phase diagram where charge and magnetic ordering occur at different critical temperatures.

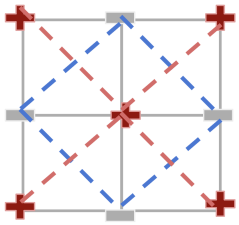

Figure 1.
The AFM ordered phase on a bipartite lattice

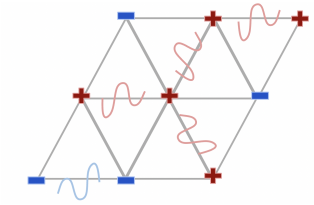

Figure 2.
Geometric frustration in the AFM case on a non-bipartite lattice

The unique AFM ordered phase on the square planar lattice is possible because the lattice is bipartite, meaning it can be decomposed into two sublattices such that each site on one sublattice borders only sites on the opposite sublattice; see Fig. 1. The situation is different for non-bipartite lattices, such as the triangular planar lattice. There is no way to arrange spins on each site of a non-bipartite lattice such that each spin only borders a spin of the opposite value, as is energetically desired in the AFM case. As such, there is no finite temperataure phase transition in the Ising model on non-bipartite lattices such as the triangular planar, as in Fig. 2 [3].

We can resolve this frustration, inducing again a finite temperature phase transition, by introducing a third spin value as described below.

A. The Ising Model

The simplest description of magnetic phase transitions is offered by the Ising model. The Ising model Hamiltonian in the absence of an external magnetic field [1]

$$E = J \sum_{\langle ij \rangle} S_i S_j \tag{1}$$

describes the energy of a collection of spins $S_i = \pm 1$ interacting on a lattice. J is the exchange interaction, and $\langle i, j \rangle$ indicates a sum over nearest neighbors. This model on the square planar lattice is exactly analytically solvable through Onsanger's method; there is a transition from the paramagnetic to the ferromagnetic (FM) phase ($J < 0$) or to the antiferromagnetic (AFM) phase ($J > 0$) at $T_c/|J| = 2.26918$.[2].

B. The Blume-Capel Model

In this paper we explore a generalization of the Ising model that includes vacancies, known as the Blume-Capel model [4, 5] on a triangular lattice. That is, we allow $S_i = \pm 1, 0$, with an additional chemical potential D which controls the balance of vacancies to filled sites:

$$E = J \sum_{\langle ij \rangle} S_i S_j + D \sum_i S_i^2 \tag{2}$$

The first term has the same interpretation as in the Ising model. The quantity S_i^2 can be interpreted as a local charge density operator with $S_i^2 = 1$ being a "charge" at site i and $S_i^2 = 0$ as a vacancy. We focus on the antiferromagnetic case, $J > 0$. The properties of the Blume-Capel model

are well-determined on the square lattice, which has been studied with Monte Carlo simulations [6–9], renormalization group methods [10, 11], and series solution expansions [12]. The phase diagram of this model consists of both a first order discontinous phase transition and a second order continuous phase transition, with the exact position of the tricritical point, at which the two types of transition meet, at $(T/J, D/J) = (0.609(4), 1.965(5))$ [13].

Our goal is to explore the less-studied features of the BC model which appear in the presence of geometric frustration, specifically focusing on the triangular planar lattice.

We will compare our numerical Monte Carlo method against Mahan and Girvin [14], who determined the phase diagram for the antiferromagnetic Blume-Capel model on a triangular lattice via a real-space renormalization group analysis. Like the square planar BC results, their phase diagram consists of a second-order transition at low D/J that becomes a first-order transition at a tricritical point $(T/J, D/J) = (0.37, 1.5)$. The major differences are the location of the tricritical point at a lower value of both D and T than the square planar lattice, and the phase boundary crossing $(T/J, D/J) = (0, 0)$, which is not the case in the square planar.

As an additional check, we compare a limiting case of our method to a known series solution of the Ising model on a honeycomb lattice [15].

In studying the BC model, our goal is to gain insight to the physics of charge and magnetic ordering on a frustrated lattice and provide insights on ordered phases that might arise in quantum fermionic models with charge and magnetic degrees of freedom.

METHODS

C. Monte Carlo

We choose to apply a classical Monte Carlo treatment to our model, Eq. (2). We work separately in the canonical ensemble (CE), assuming no particle exchange with the reservoir and thus no change in the number of occupied sites as measured by S_i^2, and grand canonical ensemble (GCE), allowing particle exchange and thus a dynamic S_i^2. In the CE the numbers of up, down, and vacancy sites are fixed to $N_\uparrow = N_\downarrow = N_0 = N/3$, while in the GCE, no restriction is imposed on the site type count and the filling fraction is controlled by the parameter D in the Hamiltonian.

Our Monte Carlo algorithm begins with an initialized state, with a single spin value assigned to each lattice site. We choose to initialize the lattice to the AFM preferred phase, with a vacancy at every third lattice site surrounded by alternating assignments of $S_i = \pm 1$; then, a change in the state is proposed. In our GCE Monte Carlo algorithm, for instance, the change is a random selection of any possible spin state of a single lattice site. From this change, we calculate a discrete change in energy using Eq. (2). Then, following the Metropolis-Hastings algortihm, this proposed change is accepted with a probability weighted by the Boltzmann distribution [1]:

$$P = min(1, e^{-\beta \Delta E}) \tag{3}$$

Where $\beta = \frac{1}{T}$ in units where we take $k_B = 1$. After the change is either accepted or denied, any quantities of interest, which are outlined in the following subsection, are measured. This repeats for a certain number of iterations, and the average value of each quantity over the course of the Monte Carlo simulation is calculated.

We perform 100 total simulations of 10^9 Monte Carlo steps each on a 15×15 periodic lattice, and compute the average values of selected observables as discussed below.

D. Observables

Monte Carlo treatments in the CE tend to utilize critical points in the average energy and magnetization, by the fluctuation-dissipation theorem, to identify the temperature T_c/J at which a phase transition occurs [1]. However, to attempt to recreate Mahan and Girvin's RG analysis results, and probe the full phase space of both T_c and D, I work in the GCE. Additionally, in order to attempt a distinction between charge order and magnetic order, we introduce more novel operators.

The filling fraction $\langle n \rangle = \langle S_i^2 \rangle$ measures the average fraction of sites on the lattice that are occupied at a given T_c and D, making it sensitive to charge order but insensitive to magnetic order.

In the present BC model in a triangular lattice at 2/3-filling, an antiferromagnetic pattern in which holes reside in one sublattice (let's call it s_0) and spins up in sublattice s_+ and spins down in sublattice s_- (see Fig. 3), a closed loop observable Z, defined below, will be highly sensitive not only to the confinement/deconfinement of the holes in sublattice s_0, but also to magnetic order:

$$Z = \prod_{i \in s_+ \cup s_-} S_i \tag{4}$$

Non-local observables like Z and similar loop observables in the toric code [16], are usually used to characterize topological phases of matter in quantum mechanical Hamiltonians [17]; however, these can be incorporated in classical spin models [18], and provide a useful and sharp tool to characterize the nature of the phase transition. In the AFM ordered phase, S_i when $i \in s_+ \cup s_-$ will only take the values $\{1, -1\}$. If the chosen sites i over which the product is taken form a null-homotopic loop– that is, a closed loop that never fully winds around the 2-torus formed by identifying opposite edges of the lattice in accordance with our period boundary condition convention– then Z will return the same value of $Z = -1$ regardless of how the loop is stretched or deformed [19]. As one crosses T_c, this measure should decay exponentially with loop length, and rapidly approach zero in the disordered phase.

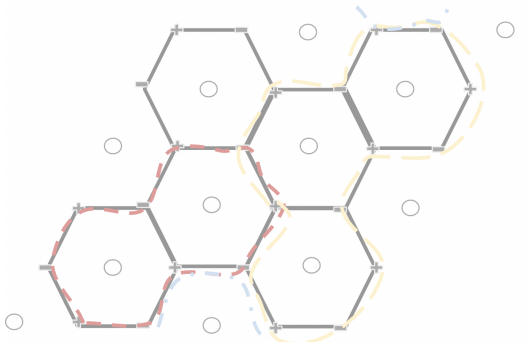

Figure 3.
Each of the three coloured sketched loop operators Z will return the value $Z = -1$ in the AFM ordered phase.

We can also construct a coordination number operator C, which is sensitive to just charge, rather than magnetic, order:

$$C = \frac{1}{6} \sum_{i \in s_+ \cup s_-} S_i^2 \tag{5}$$

This will return a value of $C = 1$ not only in the AFM ordered phase, but in any honeycomb-lattice phase regardless of the magnetic order within the honeycomb itself. Thus, the value of T_c at which the value of C decays can be compared to the value of T_c obtained from Z in order to determine whether charge order persists longer than magnetic order.

RESULTS

E. Grand Canonical Ensemble

We compare our GCE results against the upper panel of Figure 1 of Mahan and Girvin's RG analysis [14], represented in Figure 6 of our paper. Their analysis points out that the preferred AFM ordering has one sublattice occupied with $S = 1$ spins, another with $S = -1$ spins, and the third with $S = 0$; this is as we predicted as well. They report a first-order phase transition at above $D/J \sim 1.5$ and below $T/J \sim 0.37$; we see this in Figs. 4 and 5 in the sudden jumps in all measured observables at these coordinates. All observables, regardless of the type of order they are sensitive to, agree on this set of points. The second-order phase transitions are more subtle; to identify them, their derivative with respect to temperature is taken, smoothed, and analyzed to ensure axis crossing at $T = 0$. We focus on locating the maximum on the low-T peak. The results from three types of non-local operators, plotted against Mahan and Girvin's RG analysis results, are shown in figure 6.

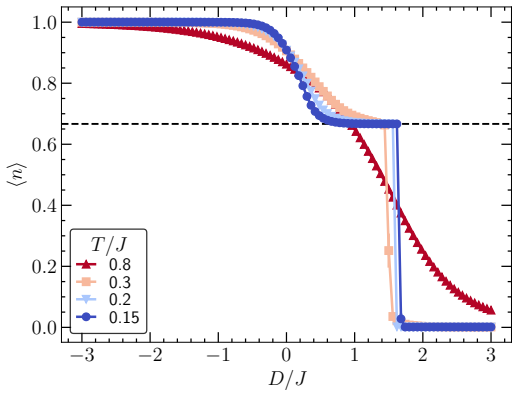

Figure 4. Filling fraction $\langle n \rangle$ as a function of D for different temperatures T/J. A (first order) jump from an empty lattice $\langle n \rangle = 0$ to $\langle n \rangle = 2/3$ occurs with decreasing D for T/J below $T/J \sim 0.37$.

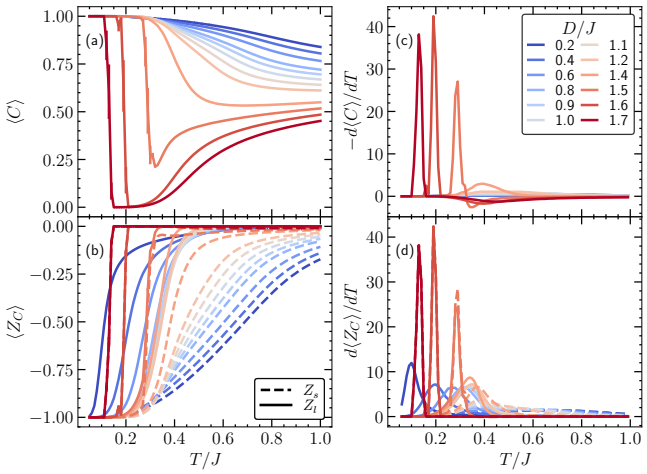

Figure 5. Non-local observables. (a) Coordination number operator. (b) Loop operator. Dashed (solid) lines correspond to short (long) loops. (c-d) Derivatives of non-local observables with respect to T.

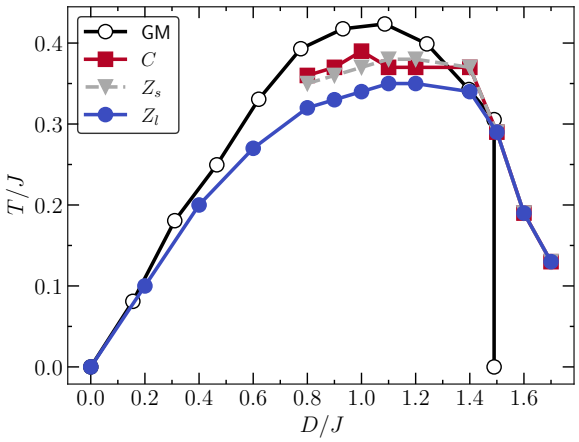

Figure 6. T/J vs D/J phase diagram. Open circles correspond to a digitized version of Ref. [14]. Location of the peak in the derivatives from Fig. 5 correspond to coordination C (red squares), short loop Z_s (gray triangles) and long loop Z_l (blue circles).

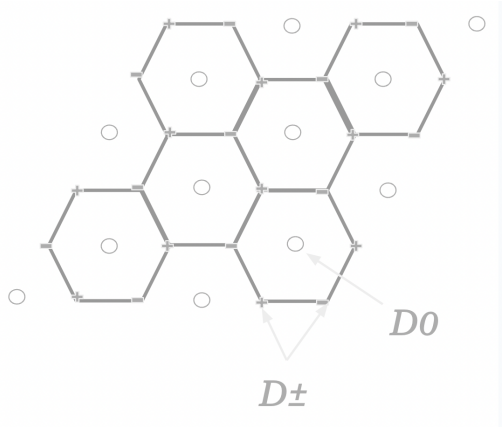

Figure 7. A demostration of sublattice-dependent potential tuning to recover the honeycomb Ising limit.

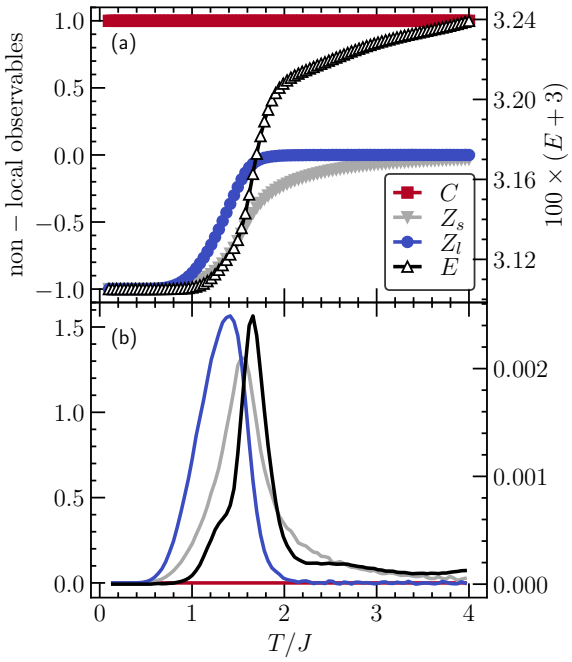

Figure 8. Results in the honeycomb Ising limit for the value of different non-local observables (top panel) and their derivatives with respect to temperatue (bottom panel). These are obtained with $D_{\pm}/J = -1000$ and setting $D_0/J = 1000$.

F. Sublattice Tuning

By tuning the chemical potential D in Eq. (2) to an arbitrarily large positive value on every third site, and an arbitrarily large negative value on all other sites, we recover the Ising model on a honeycomb lattice as shown in Fig. 7. A The known series solution for the Ising model on a honeycomb lattice yields $T_c/J = 1.51865..$ as per Table 1 in Ref. [15]. This value is significantly larger than the peak T_c in our BC model phase diagram as the forced honeycomb lattice occupancy is naturally bipartite, for which an AFM ordered phase is more energetically favorable and persists longer to higher temperatures. The average of our short loop operator Z_s, see Fig. 8, yields roughly $T_c/J = 1.51..$; less precise than that obtained in the series solution but with good agreement. As before, the long loop operator Z_l is much more sensitive to disorder and results in a lower calculated T_c. Finally, interestingly, the critical point in the average energy E overshoots the T_c/J value from the series solution.

I. CONCLUSIONS

In cuprate superconductors, the introduction of holes in a parent antiferromagnetic state leads to intricate stripe order. The question of whether one type of order, charge or spin, drives the other is still under investigation[20].

In this paper we have studied a classical model with similar qualitative features. Specifically, it allows for the formation of charge order, a regular pattern of occupied sites on a lattice, through an explicitly magnetic interaction energy. In our case, charge order arises through an avoidance of the magnetic frustration present in the fully occupied (Ising model) triangular lattice. This avoidance is allowed by vacancies occupying one of three sublattices, leaving occupation on a remaining 2/3 of the sites forming a bipartite honeycomb geometry. Our measurements support this: the low temperature limit of the filling fraction $\langle n \rangle$ is 2/3, and the coordination number operator $\langle C \rangle$ goes to 1, evidence that only the honeycomb sublattice $s_+ \cup s_-$ is occupied, and that it is occupied completely. The low temperature limit of $\langle Z \rangle$, regardless of loop length, is -1 as expected; so, spins alternate up and down on the honeycomb sublattice. Interestingly, however, the longer loop operator breaks down much faster than the short loop or coordination number. This could be a sign that perfect magnetic ordering arises only after charge order; however, it is not definitive as the short loop operator seems to track the coordination number operator quite closely. Regardless, the triangular lattice carries rich physics, and is a good candidate for further numerical study with, for instance, quantum mechanical models. A number of interacting Fermi-systems on a two-dimensional triangular lattice have been discovered that are linked to superconductivity in experiment; one class of doped cobaltates have magnetic and charge ordered phases found along with superconductivity when the material is hydrated [21–23].

Acknowledgments

This work was supported by the NSF REU program, NSF Division Of Physics, Award No. 2150515. EIGP and RTS were supported by the grant DE-SC0022311 funded by the U.S. Department of Energy, Office of Science.

[1] E. Ibarra-García-Padilla, C. G. Malanche-Flores, and F. J. Poveda-Cuevas, The hobbyhorse of magnetic systems: the Ising model, Eur. J. Phys. **37**, 065103 (2016).

[2] L. Onsager, Crystal statistics. i. a two-dimensional model with an order-disorder transition, Physical Review **65**, 117 (1944).

[3] G. H. Wannier, Antiferromagnetism. the triangular Ising net, Phys. Rev. B **7**, 5017 (1973).

[4] M. Blume, Theory of the first-order magnetic phase change in UO_2, Phys. Rev. **141**, 517 (1966).

[5] H. Capel, On the possibility of first-order phase transitions in Ising systems of triplet ions with zero-field splitting, Physica **32**, 966 (1966).

[6] Y.-L. Wang, F. Lee, and J. Kimel, Phase diagrams of the spin-1 Ising Blume-Emery-Griffiths model: Monte Carlo simulations, Physical Review B **36**, 8945 (1987).

[7] C. Care, Microcanonical Monte Carlo study of a two-dimensional Blume-Capel model, Journal of Physics A: Mathematical and General **26**, 1481 (1993).

[8] M. Deserno, Tricriticality and the Blume-Capel model: A Monte Carlo study within the microcanonical ensemble, Physical Review E **56**, 5204 (1997).

[9] P. D. Beale, Finite-size scaling study of the two-dimensional Blume-Capel model, Physical Review B **33**, 1717 (1986).

[10] A. N. Berker and M. Wortis, Blume-Emery-Griffiths-Potts model in two dimensions: Phase diagram and critical properties from a position-space renormalization group, Physical Review B **14**, 4946 (1976).

[11] T. W. Burkhardt, Application of Kadanoff's lower-bound renormalization transformation to the Blume-Capel model, Physical Review B **14**, 1196 (1976).

[12] D. Saul, M. Wortis, and D. Stauffer, Tricritical behavior of the Blume-Capel model, Physical Review B **9**, 4964 (1974).

[13] J. Xavier, F. Alcaraz, D. P. Lara, and J. Plascak, Critical behavior of the spin-3/2 Blume-Capel model in two dimensions, Physical Review B **57**, 11575 (1998).

[14] G. D. Mahan and S. M. Girvin, Blume-Capel model for plane-triangular and fcc lattices, Phys. Rev. B **17**, 4411 (1978).

[15] G. Wysin and J. Kaplan, Correlated molecular-field theory for ising models, Physical review. E, Statistical physics, plasmas, fluids, and related interdisciplinary topics **61**, 6399 (2000).

[16] A. Kitaev, Fault-tolerant quantum computation by anyons, Annals of Physics **303**, 2 (2003).

[17] M. A. Levin and X.-G. Wen, String-net condensation: A physical mechanism for topological phases, Phys. Rev. B **71**, 045110 (2005).

[18] Z. Wang and K. R. A. Hazzard, Topological correlations in three-dimensional classical ising models: An exact solution with a continuous phase transition, Phys. Rev. Res. **5**, 013086 (2023).

[19] This is easy to see: consider the simplest possible loop constructed on the sublattice $s_+ \cup s_-$. This simplest loop is one hexagon, with three vertices in sublattice s_+ and three in sublattice s_-. Thus, the product over these six sites yields $Z = -1$ as there is an odd number of sites with value $S_i = -1$. It can then be shown that any stretching of this hexagonal loop will add an even number of sites in each sublattice s_+ and s_-, and thus there will always be an odd number of sites with $S_i = -1$.

[20] B. Xiao, Y.-Y. He, A. Georges, and S. Zhang, Temperature dependence of spin and charge orders in the doped two-dimensional Hubbard model, Phys. Rev. X **13**, 011007 (2023).

[21] K. K. Takada, H. Sakurai, E. Takayama-Muromachi, F. Izumi, R. A. Dilanian, and T. Sasaki, Superconductivity in two-dimensional coo_2 layers, Nature **426**, 53 (2003).

[22] M. L. Foo, Y. Wang, S. Watauchi, H. W. Zandbergen, T. He, R. J. Cava, and N. P. Ong, Charge ordering, commensurability, and metallicity in the phase diagram of the layered na_xcoo_2, Phys. Rev. Lett. **92**, 247001 (2004).

[23] S. Zhou and Z. Wang, Charge and spin order on the trianglar lattice - na_xcoo_2 at $x = 0.5$, Phys. Rev. Lett. **98**, 226402 (2007).